Peace. *Journal of Southern Hemisphere Earth Systems Science* (2017) 67:2, 79-106. DOI: 10.22499/3.6702.002

Meteorological drivers of extreme fire behaviour during the Waroona bushfire, Western Australia, January 2016

Mika Peace[1,3], Lachlan McCaw[2], Bradley Santos[1], Jeffrey D. Kepert[1,3], Neil Burrows[2] and Robert J. B. Fawcett[1]

[1] Bureau of Meteorology, Australia
[2] Department of Parks and Wildlife, Western Australia
[3] Bushfire and Natural Hazards Cooperative Research Centre, Melbourne, Australia

(Manuscript received July 2017; accepted November 2017)

The Waroona bushfire burnt 69,000 ha south of Perth in January 2016. During the first two days of the fire, there were two pyrocumulonimbus (pyroCb) events and two destructive evening fire runs. Over 160 homes were destroyed and there were two fatalities. This case study examines in detail the links between the meteorological observations and the fire behaviour reconstruction.

The first pyroCb developed on Wednesday 6 January 2016, when the fire made an unexpectedly fast run in light prevailing winds. The pyroCb produced lightning strikes that ignited a new fire downwind of the main head fire. A second pyroCb developed on Thursday morning, against normal diurnal thunderstorm trends. Similar to the previous evening, the fire spread faster than expected, given the near-surface meteorological conditions.

On both evenings there were destructive ember storms over the towns of Waroona (Wednesday) and Yarloop (Thursday). Examination of the meteorological observations has linked these ember showers to the onset of downslope winds, locally known as `scarp winds'. As downslope winds are associated with strong localised turbulence, they provide a mechanism for transport of large numbers of firebrands.

The periods of extreme fire behaviour at Waroona were against normal diurnal expectations and did not coincide with the highest observed Fire Danger Index (FDI) values, which occurred at around 1600 LT. This study links both pyroCb events to accelerated fire spread, which presents a hazard to firefighters that is not accounted for in traditional, surface based methods of fire prediction. Downslope winds similar to those that impacted the Waroona fire occur at many locations. They provide a highly localised mechanism for destructive evening ember showers.

This investigation into the Waroona fire describes the potential impacts of fire-atmosphere feedback processes. Consequently, it highlights the need for predictive methods and tools that anticipate fire behaviour which is not steady-state. Planned simulations using a coupled fire-atmosphere model will allow further insights into features of this case study.

Corresponding author: Mika Peace, Bureau of Meteorology, South Australia
Email: mika.peace@bom.gov.au

1. Introduction

The Waroona fire burnt a total area of 69,165 ha of land and 166 houses southwest of Perth in January 2016. This study examines four critical periods of extreme fire activity during the first two days of the fire: two pyrocumulonimbus (pyroCb) events and two evening ember showers. On the evening of 7 January, when fire activity increased unexpectedly there were two fatalities and numerous homes burnt in the town of Yarloop.

Three reports have been prepared on the Waroona fire. 1) The Bureau of Meteorology report (Bureau of Meteorology, 2016b), which documents the meteorological conditions. The report includes observational data and the weather forecasts issued during the event. 2) The Department of Parks and Wildlife Report (McCaw et al., 2016), which presents a reconstruction of the fire spread and behaviour and 3) The Special Inquiry Report (Ferguson, 2016), commissioned by the Western Australian Government to examine the agency and community response and make recommendations for change. This study builds on the first two reports, but while the Bureau of Meteorology (2016b) and McCaw et al. (2016) reports each give a separate factual account of the meteorology and fire reconstruction, here we aim to explore the overlaps in order to enable deeper insights and identify lessons that can be applied to future fire meteorology training and real time decisions. Greater detail on aspects of the meteorology and fire reconstruction are contained in the above reports and interested readers are directed there.

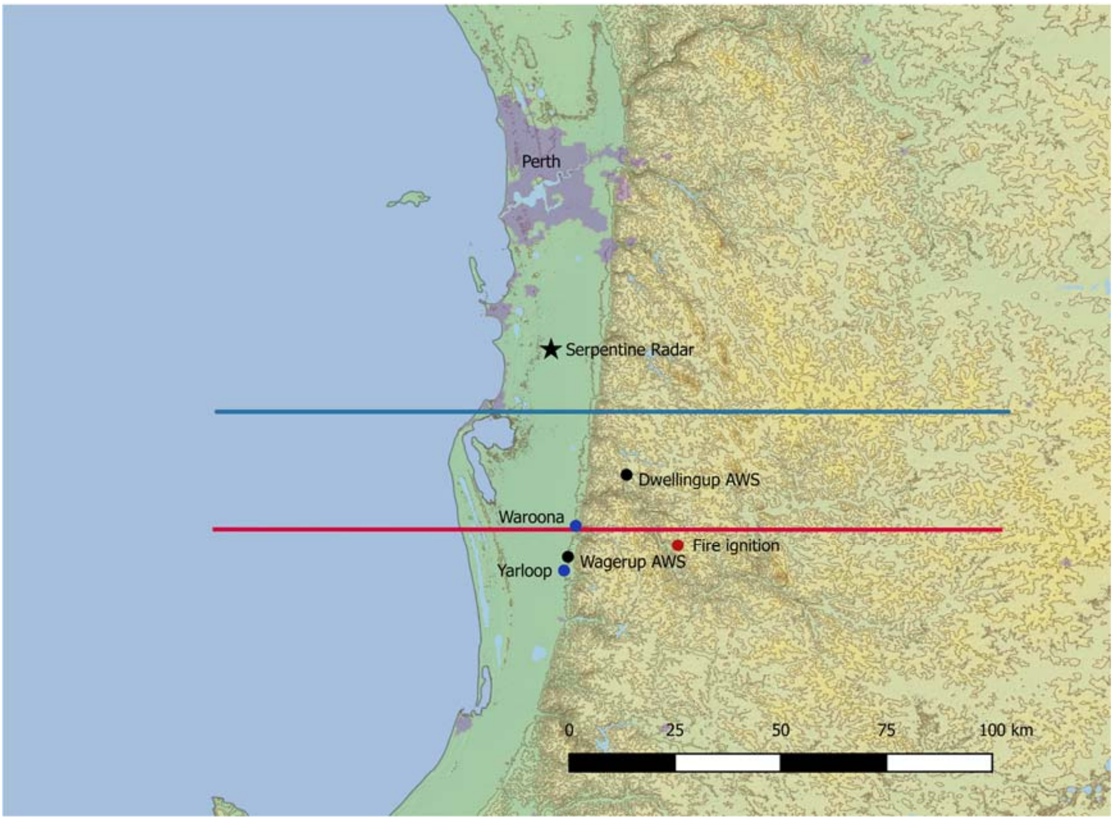

Fig. 1: Map showing the fire region with fire ignition point, AWS, radar and town locations. Topography (shaded) shows the extent and sharp western boundary of the Darling Scarp. Blue line shows the cross section in Fig. 6 and red line shows the cross section in Figs. 11 and 12.

The Waroona fire was ignited by a lightning strike on 5 January 2016 and first identified around 0630 LT (Local Time) on 6 January. Figure 1 shows the area surrounding the fire and Table 1 gives a timeline of the key events described in this study. During the first two days (6 and 7 January), winds were generally east to north-easterly and the fire was running from east to west through heavy fuels on the Darling Plateau, which has an escarpment on the western side. After 7 January, the fire continued to burn for several days across the coastal plain through a mosaic of mostly lower fuel loads; during this period, easier access and lower fire intensities facilitated suppression activities. Figure 2 shows the reconstruction of the fire spread (modified from McCaw et al. (2016)). This study focuses on the first two days of the fire.

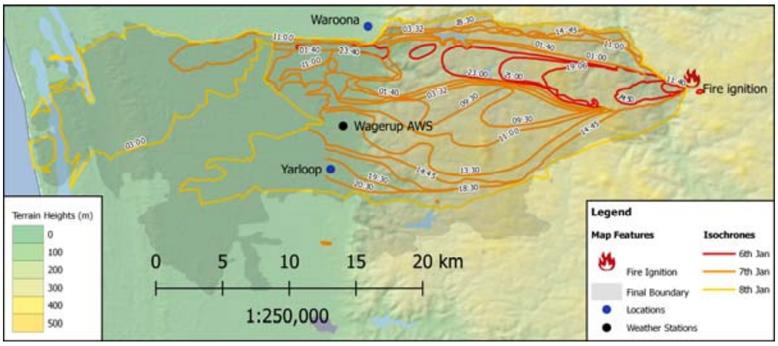

Fig. 2: Reconstruction of the spread of the Waroona fire, modified from McCaw et al. (2016). This case study focusses on the first two days of the fire (red and orange isochrones show 6 and 7 January respectively).

Antecedent conditions were dry, with low rainfall from May to October 2015 and above average temperatures. Consequently, soil moisture was low and fuels across the landscape, including heavy (> 6 mm diameter) fuels were very dry. The dominant vegetation types were jarrah (*Eucalyptus marginata*) and marri (*Corymbia calophylla*) forest, with areas of bullich (*Eucalyptus megacarpa*), blackbutt (*Eucalyptus patens*) and wandoo (*Eucalyptus wandoo*). Parts of the vegetation burnt during the first two days were in a current and rehabilitated bauxite mining site. Detailed descriptions of the fuels and the dominant vegetation types at different stages of the fire are contained in McCaw et al. (2016).

Table 1: Timeline of events during the Waroona fire.

Tuesday 5 January	
Evening	Lightning ignition of Waroona fire
Wednesday 6 January	
0630 LT	Fire first identified on satellite imagery
1600LT	Sea breeze passage at Waroona AWS
1612 LT	Onset of lightning from pyroCb
1614 LT	FFDI peak of 40
1800-1906 LT	Very rapid fire spread 3300 m s^{-1}
2038 LT	Last lightning strike
2100 LT	Sustained ember attack reported at Waroona
1900-2300 LT	Fire spread driven by mass spotting
Thursday 7 January	
0700-0800 LT	Major fire run on southern flank starts
Late morning	Extensive crown fire activity
1120-1200 LT	PyroCb pulse 1
1330-1417 LT	PyroCb pulse 2
1417 LT	Last lightning strike
1613 LT	Peak FFDI of 54
1900-2030 LT	Ember storm over Yarloop
1933 LT	Radar shows doubling of plume height

Juxtaposed against the large burnt area and the significant impacts of the Waroona fire, conditions as assessed by Australian operational fire danger metrics were not severe for most of the period. At Dwellingup (the closest Bureau of Meteorology AWS to the fire area) a daily maximum FFDI[1]>= 50 has been recorded on 17 occasions from 1999 to mid-2016 (from AWS data recorded at 30 minute intervals). This includes an observation of FFDI 54 during the Waroona fire event on 7 January (T = 39.2°C, Td=3.4°C, RH=11 per cent and easterly winds 23 km h^{-1}). The timing of the FFDI 54 observation was 1613 LT, which is significant as it did not coincide with any periods of significant fire activity or fast fire spread. So, as seen at other fires (particularly where plume development featured) (e.g. Peace et al. (2015b)) there was little correlation between highest FFDI and extreme fire behaviour.

This timing discrepancy between max FFDI and the observed extreme fire activity highlights a need in Australia for better methodologies for interpreting and contextualising weather information pertinent to fire prediction. It is widely recognised within the community of fire practitioners and researchers that traditional methods of calculating and measuring fire suppression potential and fire perimeter growth using surface inputs and assuming quasi-steady state behaviour are limited in many circumstances. Particular examples of where current methods are limited include capturing processes such as plume development, pyroCb, ember storm development, local topographically forced winds and interactions between these elements, all of which featured in the Waroona fire.

This case study is structured in sequence, following the four extreme fire behaviour events. The methods are described next, then the pyroCb event during the late afternoon of 6 January, which leads into the second phase; the ember shower over Waroona the same evening. The next section examines the pyroCb event during the morning and early afternoon of 7 January and finally we discuss the conditions during the evening of 7 January, when the town of Yarloop was destroyed. The paper is constructed in sections that consider each period separately and the conclusions consider how the findings may be applied to future events.

2. Methods

This report draws on a range of meteorological data from the fire, including Automatic Weather Station (AWS) data, satellite imagery, radar data and output from high resolution Numerical Weather Prediction (NWP) simulations. The closest AWS stations are Dwellingup and Wagerup. The Dwellingup AWS is a Bureau of Meteorology station, but its anemometer is at a non-standard height of 29 m so as to be above the tree canopy. The Wagerup AWS is owned by the mining company Alcoa and located next to the refinery. Its primary purpose is monitoring conditions (particularly wind) for the alumina refinery and smelter emissions. The meteorology near the Wagerup refinery is complex due to the influence of the Darling Scarp and strong local variability is seen in near- surface and above-surface winds. This variation is documented in Department of Environment and Conservation (2011), which examines air quality at towns nearby the refinery. As the Wagerup instrumentation is not a standard Bureau of Meteorology AWS, Fire Danger Index (FDI) values are not quoted for this site. Satellite data from Himawari and MODIS satellites capture the periods of pyroCb. The Serpentine Radar is a C-band 5 centimetre wavelength Doppler radar that scans every 6 minutes and is located 50 km north of Waroona. The radar provides insights into the structure of the pyroCb episodes as well as the evening ember showers.

Our exploration of the observed meteorology is supplemented by some very high resolution hindcasts or simulations of the meteorology, generated by a research version of the numerical weather prediction model (the Australian Community Climate and Earth System Simulator or ACCESS) used operationally at the Bureau of Meteorology in its routine weather prediction activities. The research version of ACCESS uses the UK Met Office's Unified Model (version 8.5) for its atmospheric component. Three simulations were performed, initialised at 1500 UTC on 5 January and 0300 UTC and 1500 UTC on 6 January 2016. Each simulation consisted of a global model simulation together with successive limited-area nested model runs with grid spacings of around 4 km, 1.3 km and 400 m over progressively smaller regions. The nesting is one-way, with information only owing from the larger-grid-spacing nests to the smaller-grid-spacing nests. The simulations do not simulate the fire.

Through this report, time is shown as local time (LT) to simplify reconciling fire activity with diurnal trends. The time zone in Western Australia is UTC +8 hrs, with no daylight saving (sunrise and sunset consequently occur `earlier' than in eastern Australian states).

[1] 1Forest Fire Danger Index (FFDI) and Grassland Fire Danger Index are the operational measures of fire risk used in Australia. FFDI is quoted in this report as it is consistent with the dominant fuel type burnt during the Waroona fire.

This case study examines the available data and makes many inferences linking the fire behaviour and meteorological observations, drawing on comparison from previous published events and simulations. It is difficult to prove definitively the processes that took place using the available data, so this study is necessarily somewhat speculative, however we aim to identify and comprehensively describe meteorological ingredients that may have contributed to the observed fire activity. The intended second phase of this study is to run coupled fire-atmosphere simulations of the Waroona fire using a fire model coupled to the ACCESS meteorological model. This will enable detailed examination of some of the hypotheses presented here. As the coupled simulations will focus on simulation results, the focus here is on observational data, and greater consideration of NWP results will be given in the follow-up study.

3. PyroCb event 1 (6 January)

The fire was first detected at 0630 LT on 6 January (see McCaw et al. (2016) for a detailed description). Satellite imagery from Himawari visible bands shows that the smoke plume developed between 1020 LT and 1140 LT, coincident with development of cumulus cloud to the north and west. By 1530 LT, overshooting pyrocumulus cloud extended above the smoke and the first lightning strikes were observed at 1612 LT (Bureau of Meteorology, 2016b). The closest (non- fire) thunderstorm activity occurred approximately 350 km to the northeast; development time was similar for both pyroCb and (non-fire) thunderstorms. Figure 3 shows the pyroCb at 1810 LT. Satellite derived brightness temperature reached -60°C, indicating an overshoot of the tropopause by reference to the 2000 LT (1200 UTC) Perth radiosonde (see Fig. 4), which was released approximately 100 km north of the fire. The radiosonde shows limited environmental moisture (apart from a shallow moist layer near 200 hPa (12 km)), strong low-level wind shear and very high Convective Available Potential Energy (CAPE) (assuming a surface temperature of 38°C and dewpoint temperature of 18°C).

Fig. 3: High resolution visible image from Himawari satellite at 1810 LT 6 January 2016.

The pyroCb development occurred near the time of the sea breeze passage. In Western Australia, sea breeze dynamics are closely linked to the west coast trough; a semi-permanent feature of the synoptic pattern during summer months (Kepert and Smith, 1992). The west coast trough extends several hundred kilometres from the summertime `Pilbara heat low' to the southwest of Western Australia. It is a mobile feature that acts as a focus for both local sea breezes and thunderstorm development under favourable environmental conditions. On the morning of 6 January, the trough was positioned offshore, consistent with development of a late sea breeze. The observations at Wagerup AWS (see Fig. 5) show that between 1600 LT and 1630 LT, winds turned from southeast to south-westerly and the temperature dropped by 4.5°C. Lightning strikes were observed between 1612 LT and 2038 LT on the Global Positioning and Tracking Systems Pty Ltd (GPATS) and ENGLN Lightning Detection System. Therefore, it is likely that the sea breeze convergence line was the trigger for electrification of the pyroCb. This is supported by the simulation results shown in Fig. 6, which shows the cooler, green area as the advancing sea breeze front, with vertical motion (black contours) located ahead of the leading edge. It is also consistent with observations of leaf freeze, as the orientation of scorched leaves and twigs indicated a south to south-westerly wind direction (McCaw et al., 2016).

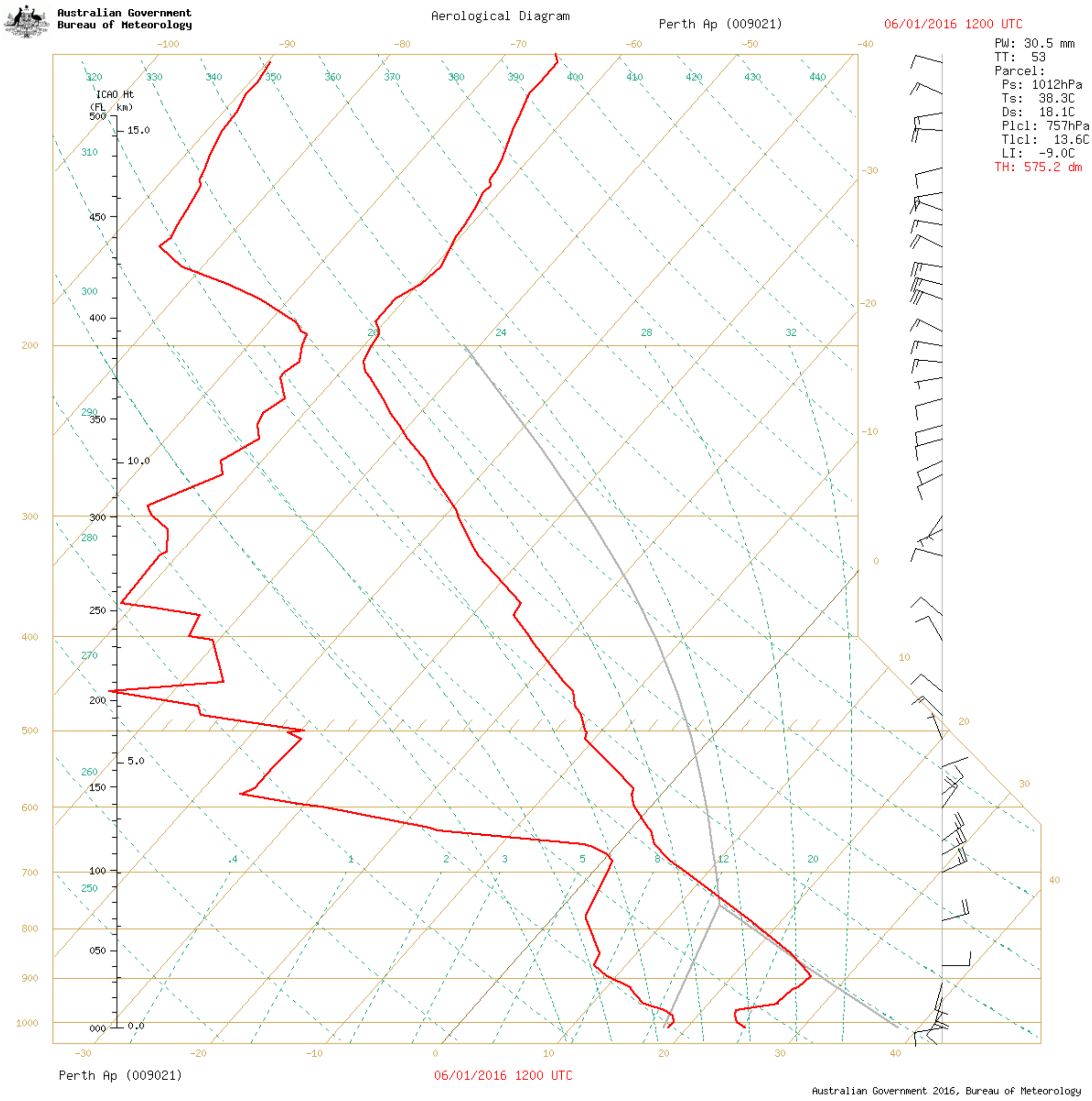

Fig. 4: Radiosonde from Perth Airport 2000 LT 6 January 2016.

The pyroCb was mostly surrounded by clear air and therefore easily visible. The latter stages of the pyroCb were recorded on time-lapse video between 1845 and 1945 LT by Darren McCagh of Farmhouse Films. His footage shows a number of features; a still from the video is shown at Fig. 7. The video shows that the main plume is highly turbulent, exhibiting rotation consistent with the strong backing vertical shear seen on the 2000 LT (1200 UTC) Perth Airport radiosonde. A shear layer approximately halfway up the vertical extent of the plume produces a shelf cloud just before sunset. Two main cirriform anvils and a remnant anvil pulse indicate that the pyroCb was multicellular (the multicellular nature is also evident in Fig. 3). As sunset approaches, mammatus develops in the middle and upper levels of the cell (sunset was at 1928 LT and civil twilight 1957 LT).

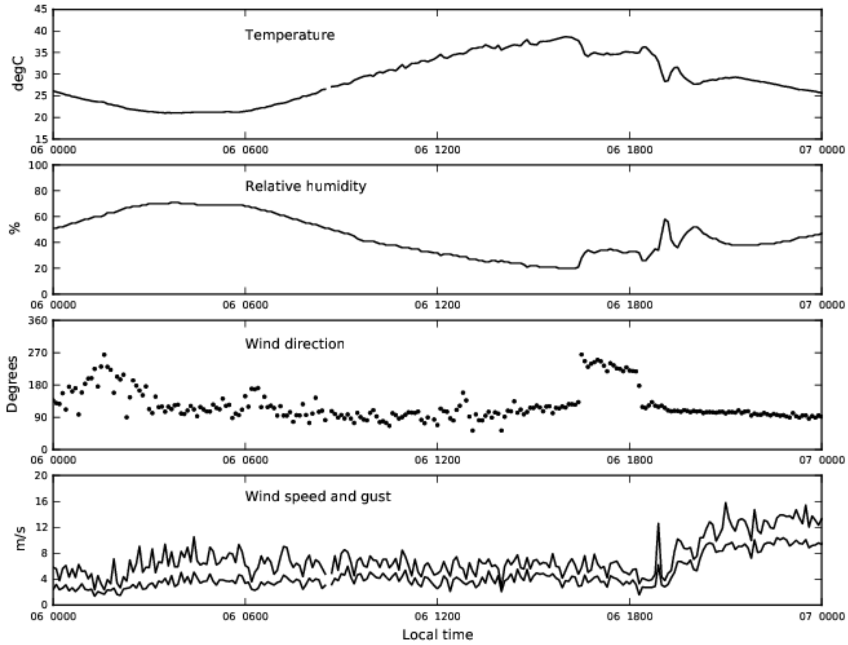

Fig. 5: Observations from Wagerup Automatic Weather Station from midnight 6 January to midnight 7 January 2016.

Between 1800 and 1906 LT the fire underwent a period of very rapid spread through 37 year old fuel. McCaw et al. (2016) state that the observed rate of spread between 1800 and 1906 LT is inconsistent with the light winds recorded on nearby AWS, even allowing for heavy fuels. This fast spread period (observed rate of spread 3300 m h^{-1} on an uphill slope) is coincident with strong convective development and the peak lightning period between 1830 and 1930 LT (when numerous videos and photographs were taken). Estimated fireline intensity during the peak spread period is of the order of 40,000 kW m^{-1}, assuming a fuel load of 25 t ha^{-1}. The fast spread period corresponds to the cessation of the sea breeze and transition to easterly winds. Light surface winds were recorded at all nearby AWS through this period. Between 1800 and 1900 LT wind speed averaged 11.5 km h^{-1} at Wagerup and 8.6 km h^{-1} at Dwellingup.

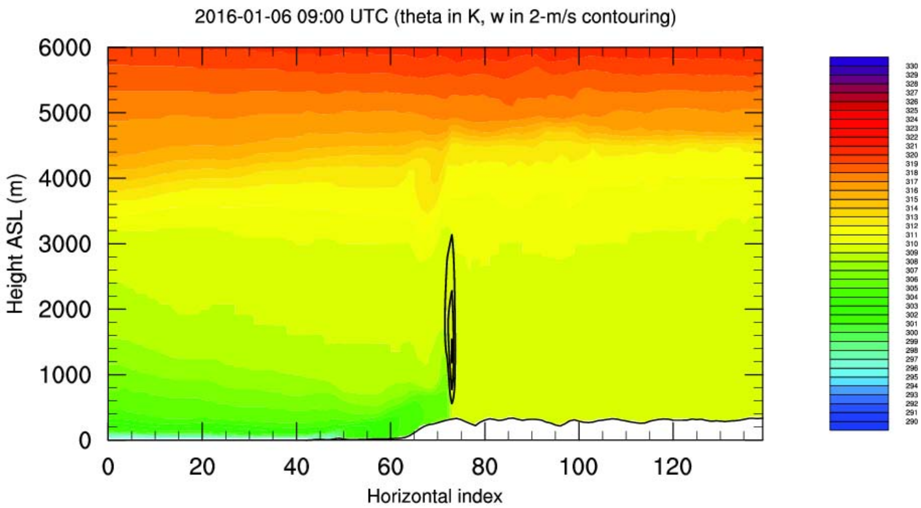

Fig. 6: High resolution ACCESS simulations showing cross section of vertical velocity (2 m s^{-1}) contours, black shows upmotion and potential temperature (K, shaded) at 1700 LT 6 January. Cross section line shown in red in Fig. 1.

At Wagerup, winds were mostly around 10 km h^{-1}, however the 1854 LT report was 22.4 km h^{-1} gusting to 45.4 km h^{-1}, coincident with a temperature drop from 32.1°C to 27.9°C (offset by 6 minutes from the wind maximum) (see Fig. 5). The wind and temperature spikes are consistent with the passage of a density current produced by outflow from the pyroCb. A pyroCb downdraft core can be seen on Serpentine radar at 1755 LT (Fig. 8). The high reflectivity low level echoes are located just south of Wagerup at 1842 LT (Fig. 9). The radar signature is consistent with warm rain processes, with weaker elevated echoes (due to high concentrations of cloud condensation nuclei in the plume updraft) strengthening at low levels in the downdraft as melting ice particles coalesce into larger raindrops below the elevated freezing level at 5000 m. The pyroCb downdraft signature on radar matches the temperature drop and wind gust at Wagerup AWS at 1854 LT, although the velocity scan does not resolve a coincident wind maximum. It is worth noting that the pyroCb downdraft is located approximately 15 km from the fire at this time.

Fig. 7: Pyrocumulonimbus cloud over the Waroona fire. Still from video taken by Darren McCagh of Farmhouse Films at around sunset 6 January.

Rothermel (1991) describes fires as being either `plume driven' or `wind driven'. The Waroona fire between 1800 and 1900 LT on 6 January was clearly plume dominant. Rothermel (1991) further separates plume driven fires as having two mechanisms for movement; the first is caused by momentum feedback from the vertical velocity in the convection column increasing turbulence in the surface winds and the second is from a downburst of wind blowing outwards at the base of a convection cell (which may be either from pyro-convection or a non-fire thunderstorm). He highlights that the second is a situation which can be extremely dangerous. It is plausible that the observed rate of spread at the Waroona fire between 1800 and 1906 LT had a contribution from the second process described by Rothermel (1991), a gust-front outflow, in this case from the pyroCb. The timing of the fire run is similar to the time of the wind maximum at Wagerup AWS at 1854 LT.

The environment was relatively dry (precipitable water 30 mm on the Perth 2000 LT (1200 UTC) radiosonde) and therefore conducive to evaporative cooling and strong outflows in downdrafts. In addition, the pyroCb was multicellular, which supports temporal and spatial separation between the updraft and downdraft.

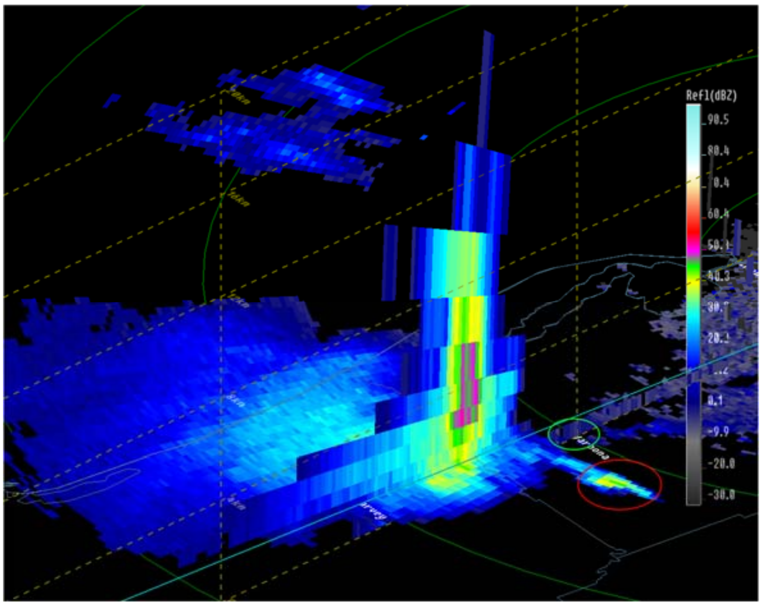

Fig. 8: 3D-Rapic combined cross-section and plan view of the pyroCb at 1755 LT 6 January. Green ellipse shows the location of Waroona and red ellipse shows the approximate surface fire location. The green and dashed brown radial lines are oriented approximately north (right) to south (left), Fig. 1 shows locations of Serpentine radar and Waroona.

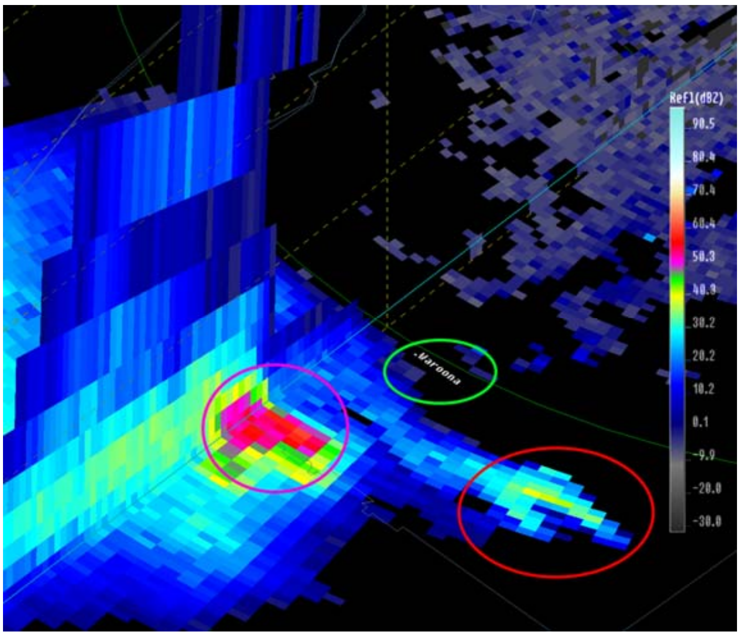

Fig. 9: 3D-Rapic combined cross section and plan view of the pyroCb at 1842 LT 6 January. The pink ellipse indicates the thunderstorm outflow and the red ellipse shows the approximate surface fire location. The green ellipse shows the location of the town on Waroona. Note the separation between the fire and outflow. The green and dashed brown radial lines are oriented approximately north (top right) to south (bottom left), Fig. 1 shows locations of Serpentine radar and Waroona.

Two eyewitnesses saw cloud to ground lightning strikes from the pyroCb ignite new fires, although no time or location was reported. The closest lightning strikes from the pyroCb to Waroona occurred approximately 4-5 km east of the town between 1612 and 2000 LT, approximately 8 km ahead of the known position of the main head fire (see Figure 17 in Bureau of Meteorology (2016b)).

We suggest that the fast fire run between 1800 and 1900 LT may have occurred due to two processes, firstly, lightning ignition by the pyroCb of one or more spot fires ahead of the main fire front and secondly, by ember transport from the lightning-ignited spot fires, driven by the pyroCb outflow gust front, producing more rapid spread than indicated by the environmental winds.

The dangers associated with thunderstorms impacting fires in Australia are well recognized, both from potential for new fire ignitions (particularly from `dry' strikes) and due to wind gusts with variable speed and direction emanating from outflow boundaries and producing erratic fire spread. Plume development at the Berringa fire, which was associated with a frontal zone is comprehensively described in Tolhurst et al. (1999) and the danger associated with convective downdrafts is highlighted in that study.

Documented examples of thunderstorm outflows impacting firegrounds in the USA include the Dude Fire (Goens and Andrews, 1998), the Yarnell Fire (Yarnell Serious Accident Investigation Team, 2013) and the Waldo Canyon Fire (Johnson et al., 2014). At the Dude Fire, a thunderstorm that developed over the fire produced a strong downburst during its decay, entrapping eleven firefighters, six of whom died. Features of the environment included mountain topography and an atmospheric profile favourable for dry microbursts. The Waldo Canyon fire featured rapid fire spread and a dramatic increase in fire intensity coincident with the passage of a gust front from a dry microburst thunderstorm outflow. At the Yarnell fire, 19 firefighters were killed due to a sudden and unexpected change in fire spread direction associated with a thunderstorm outflow (although Yarnell was not a dry microburst environment). The atmospheric profile at the Waroona fire was favourable for dry microbursts (no significant rainfall was reported at the fire ground). There is a danger to firefighters operating near either pyroCb or non-fire thunderstorms, particularly as downbursts may persist for several minutes to an hour and propagate distances of tens of kilometres from the source. Downbursts have the potential to produce rapid onset, sustained periods of anomalous and erratic fast fire spread.

The fire reconstruction report (McCaw et al., 2016) highlights the need to better understand the complex interactions between fires and atmosphere as the fast fire run could not be reconciled with surface weather observations. The Waroona fire was plume-dominated when the early evening fire run occurred. Our analysis of the available evidence suggests that a new fire was ignited by lightning from the pyroCb and it is likely this new fire was in part driven by downburst outflow from the pyroCb. This highlights the limitations of operational fire-spread predictions that rely on background environmental winds as inputs, particularly if conditions are favourable for pyroCb development.

4. Waroona ember shower

During the evening of 6 January there was another period of extreme fire behaviour, this time associated with mass spotting. Shortly after 2100 LT the Incident Management Team (IMT) Planning Officer received several reports advising that the fire was impacting the town of Waroona, and around 2100 LT a `sustained ember attack' on Waroona was reported. This came as a surprise to the IMT as latest available information placed the fire 13 km east of the town at 1900 LT. Ferguson (2016) suggests that the fire impacting Waroona was from the development of a new head fire ahead of the main front. Our analysis supports this suggestion; it is plausible that the lightning ignitions described in the previous section started a new fire between the main fire front and Waroona and the new fire was subsequently driven closer to the town of Waroona by the gust front from the pyroCb outflow.

The pyroCb itself is unlikely to be the primary mechanism for the evening ember attack on Waroona due to the time lag between the pyroCb lifecycle and the ember shower over Waroona. The final lightning strikes occurred at 2015 LT, after which time the plume would have been in a weakening phase. As the ember attack occurred from 2100 LT and the burnout time for firebrands is typically one to two minutes, (Ellis (2013) reports burnout times up to seven minutes), the ember shower cannot be readily attributed to the pyroCb plume. Additionally, vertical turbulent dispersion in the plume would contribute to spreading of lofted firebrands, and precipitation loading in the plume would contribute to extinguishing firebrands. The description of a sustained ember attack appears more consistent with large numbers of embers transported by a horizontal near-surface turbulent mechanism (with a shorter trajectory) as opposed to a more dispersed vertical mechanism, which would have a longer transport time, meaning embers would be more likely to extinguish prior to deposition. See (for example) Sullivan (2017) Fig. 8 for a pictorial representation and conceptual description of the spotting process.

The Wagerup AWS observations (Fig. 5) show a sustained increase in easterly winds from around 1900 LT. This would be a contributing factor to increased fire activity, but does not provide a direct explanation for the ember shower. The Serpentine radar velocity data at 2130 LT (shown in Fig. 10) shows a convergent zone to the southeast of Waroona. This convergent zone developed around 2055 LT at around 1 km elevation and continued for two to three hours, downwind of Waroona and coincident with the strongest reflectivity near the fire. The 2130 LT radar scan also suggests the fire is 6-7 km away from the centre of the town, closer than reported in Ferguson (2016).

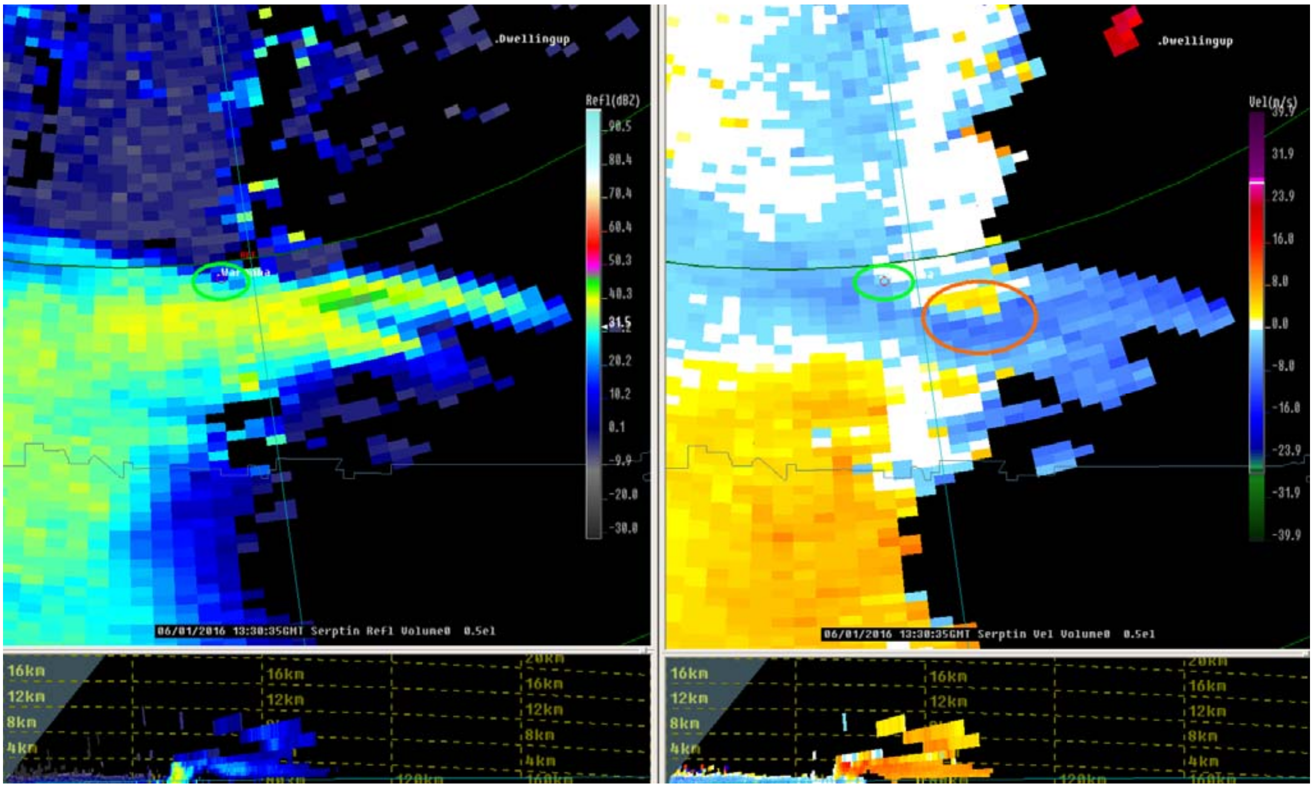

Fig. 10: 3D-Rapic plan view split image showing reflectivity (left) and velocity (right) at 2130 LT 6 January. The radar is located approximately 50 km north of the fire. Green ellipse shows the location of Waroona and red ellipse shows the convergent area southeast of Waroona. Yellow/orange/red colours show movement away from the radar, blue shows movement towards the radar.

Downslope winds are a mechanism that may have contributed in whole or in part to the ember attack on Waroona. The `scarp winds' are the well-known local occurrence of downslope winds, a meteorological phenomenon that occur in the lee of mountain ranges in many parts of the world, particularly on ranges with gentle windward and steep leeward slopes. Scarp winds are nocturnal, strong and gusty winds that develop near the base of the scarp through summer months. The local mechanism is for a synoptic easterly ow, causing air to rise to the top of the scarp from further inland, at which point it is cooler and denser than the surrounding airmass. This produces an unstable situation and consequently the air flows down the scarp as a turbulent density current.

Several Australian studies examine the mechanisms and signatures in downslope winds, with a focus on Perth (Pitts and Lyons (1989), Pitts and Lyons (1990), Blockley and Lyons (1994)) and Adelaide (Grace and Holton (1990), Sha et al. (1995)), as both capital cities have mountain ranges to the east and experience downslope winds that are occasionally severe and damaging. The winds are locally called `scarp winds' in Perth and `gully winds' in Adelaide. Unpublished high resolution simulations by Grace (pers. comm. 2012) show the location of strong winds to be highly localised in `hot spots' near the base of the lee slope of the ranges.

Hydraulic jumps are a particular feature of the downslope wind environment examined in several of the studies. The hydraulic jump is an abrupt increase in the depth of the atmospheric layer as it transitions from a higher-velocity shallow layer `squeezed' over the top of the mountain to a slower velocity, deeper layer above the coastal plain. It is a highly localised pocket of turbulent vertical motion, which, if co-located with a fire plume has the potential to enhance the plume updraft.

Krumm (1954) describes the Rattlesnake Fire in California, which spread unexpectedly downslope in the late evening, fatally burning fifteen firefighters. Although Krumm does not use the terminology `downslope winds', his detailed description of the event is consistent with the downslope wind mechanism. Krumm makes several important points relevant to the Waroona fire: firstly; the `explosive' behaviour is indicative of a change in airmass, secondly; there is high local variability in wind strength in adjacent gulches (gullies) along the base of the range and thirdly; the onset of downslope winds is sudden and not associated with any visible signs that may signal the danger.

Figure 11 shows a cross section of potential temperature and vertical motion at around the time of the ember shower. A focus of downwards vertical motion can be seen above the scarp slope. Animations also show the presence of a density current of cooler air moving from east to west across the scarp. The arrival time at Waroona of the simulated density current matches well with the reported ember shower. Density currents such as that simulated moving across the scarp typically have strong vertical motion and turbulence along the leading edge, which provides a mechanism for firebrand transport. Figure 12 shows a cross section of wind speed at the same time as Fig. 11. Of note is the wind maximum directly above the base of the scarp. The height of this maximum is well within the fire plume depth, which is seen to be around 4 km on radar.

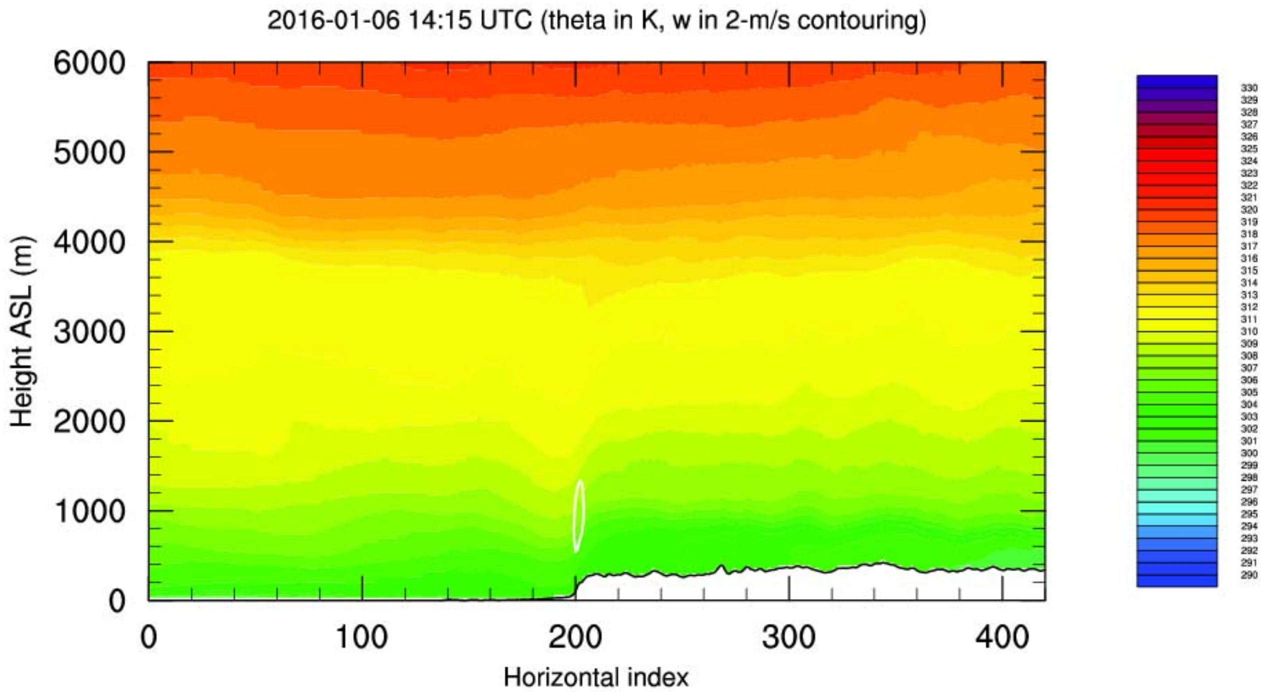

Fig. 11: High-resolution ACCESS simulation showing cross section of vertical velocity and potential temperature at 2015 LT 6 January. White ellipse indicates downmotion near the hydraulic jump. Cross section line shown in blue in Fig.1.

There are implications for enhanced fire activity for a fire located in a region of downslope winds, as they provide a clear mechanism for rapid, anomalous direction of fire spread as well as turbulent transport of firebrands and plume development. If a hydraulic jump is also present, the strong vertical motion in the jump region is an obvious mechanism for lofting and dispersal of firebrands.

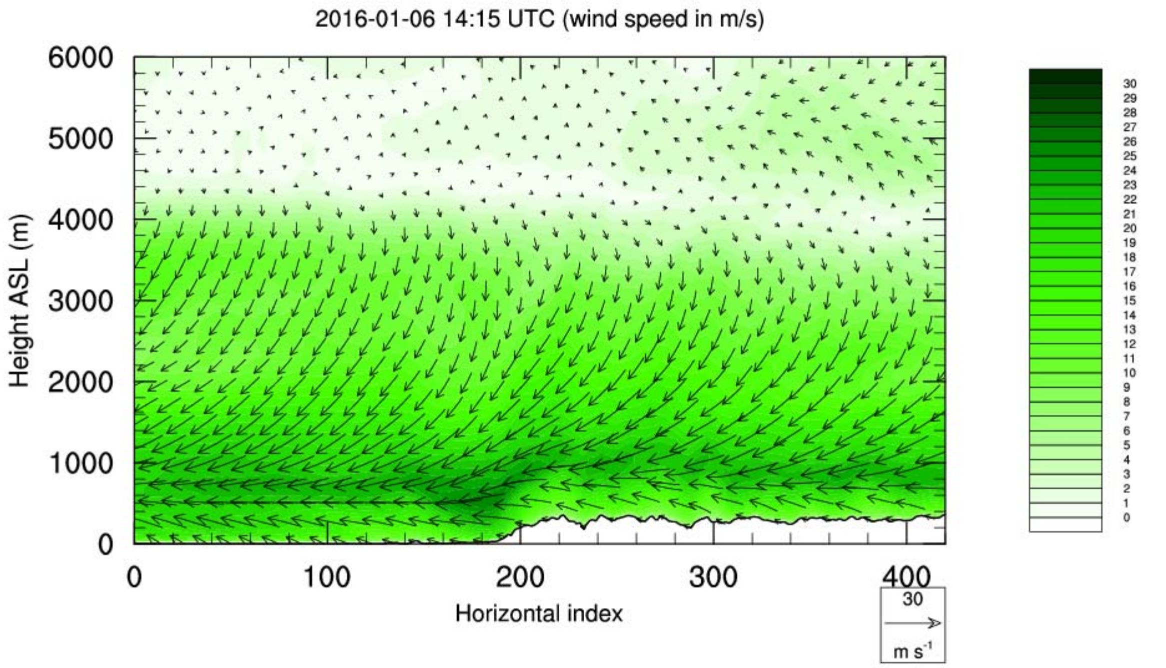

Fig. 12: High-resolution ACCESS simulation showing a vertical cross section of horizontal wind speed (u, v) at 2015 LT 6 January. Cross section line shown in red in Fig. 1.

Extreme fire activity driven by downslope winds at Waroona on 6 January is consistent with the synoptic pattern and AWS observations at Wagerup, Dwellingup and Harvey, as all sites show a sustained increase in gusty easterly winds from around sunset.

The fire reconstruction in McCaw et al. (2016) describes a separate ignition just west of Samson Brook Dam that spread westwards along the Samson Brook, with defoliation indicating an active crown fire. The description is consistent with scarp winds channelling along the Samson Brook valley.

We suggest that the sustained ember storm on the evening of the 6 January at Waroona was driven in whole or in part by ember transport driven by downslope winds and the likely source of the embers was the lightning-ignited spot fire which was closer to Waroona than the main fire front.

On 6 January, the maximum FFDI from AWS observations was not coincident with the periods of extreme fire behaviour and fast fire spread. Maximum FFDI recorded at Dwellingup was 40 at 1614 LT (Fire Danger Rating of Very High). The fastest fire spread of 3300 m h^{-1} was observed during the peak convective period, between 1800 and 1906 LT (McCaw et al., 2016), by which time FFDI at Dwellingup had reduced to nineteen and fifteen at 1800 and 1900 LT respectively (High), with winds of 13-15 km h^{-1}.

5. PyroCb event 2 (7 January)

The feature of interest during the daytime on 7 January was development of pyroCb in the late morning, earlier than normal diurnal trends of surface-based thunderstorm development. There were two separate short-lived pyroCb pulses, the first at 1130 LT and the second at 1330 LT. Figure 13 shows the plume from the second pulse being advected to the east in a high wind shear environment. The pyroCb development was preceded by a major run on the southern flank of the fire that started between 0700 and 0800 LT (McCaw et al., 2016). Satellite imagery shows smoke injected above the overnight radiation inversion as early as 0630 LT, followed by an increase in fire activity between 0730 and 0800 LT (inferred from shadows cast by smoke puffs). The timing of the increase in fire activity is consistent with observations from Wagerup AWS showing an increase in wind speed from 0720 LT, which would be associated with weakening of the overnight radiation inversion (Fig. 14).

Fig. 13: NOAA MODIS Aqua satellite image at 1355 LT 7 January showing sheared pulsed convection over the Waroona fire.

From around 0730 LT, the fire spread actively through until early afternoon, however spread direction through the morning period was inconsistent with local surface winds. During the morning, the fire was burning as a long head fire along the southern edge of the fire perimeter (see Fig. 2). However, between 0700 and 1200 LT Dwellingup AWS recorded easterly winds (70 to 100°) of 17-26 km h^{-1}. At Wagerup AWS, easterly winds averaging 20 km h^{-1} were recorded from 0700 to 0915 LT, then south-southwesterly winds around 8 km h^{-1} until 1130 LT, then north-easterly winds averaging 11 km h^{-1} through the afternoon (see Fig. 14). The morning wind observations are inconsistent with both fire spread direction (to the southwest) and rate of spread, as the reconstructed rate of spread was 1500 m h^{-1}. However, the morning fire run is consistent with the 0700 LT Perth radiosonde observations, which reported north-northeast winds (030°) with speeds of 28-82 km h^{-1} between the surface and 1550 m.

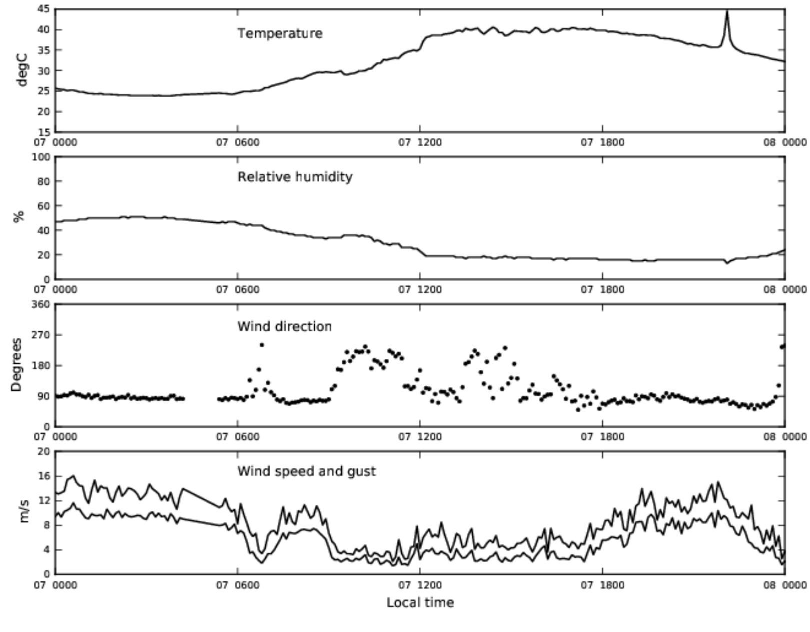

Fig. 14: Observations from Wagerup Automatic Weather Station from midnight 7 January to midnight 8 January 2016.

Potter (2012) presents a conceptual model of airflow around a developed fire front (see for example Fig. 6 in Potter (2012)), which provides an explanation for the anomalous spread. A feature of the conceptual model is the `descending rear inflow' into the back of the head fire. Potter (2012) states that the origin of the inflow is unclear and that the height from which the inflow descends will be influenced by factors including the stability, wind profile and fire geometry. Coupled fire-atmosphere simulations (Peace et al., 2016) show trajectories of elevated higher momentum air being entrained into the back of a head fire, demonstrating that energy from above the surface can affect surface fire spread. It is likely that the Waroona morning fire run was driven not by the local environmental surface winds, but by the dynamics of the plume structure entraining the elevated meteorological north-easterly low level jet into the descending rear inflow jet of the fire. This mechanism is physically consistent with the observations and reconciles with the morning fire spread.

Wagerup AWS recorded a south-westerly wind direction between 0915 and 1130 LT, opposite in direction to the synoptic east to northerly ow. This direction reversal is likely to be due to convergent inflow into the plume due to fire-modified winds. The AWS observation site was 2-4 km southwest of the head fire at this time, which is consistent with the simulated spatial scales of fire-modified winds shown in Peace et al. (2015a). This is confirmed by the Serpentine radar data shown in Fig. 15, which shows convergence along the fire front extending up to 5 km ahead of the fire at 1130 LT. The AWS and radar observations provide rare direct evidence of the spatial and temporal extent and strength of the fire-modified winds, a process that is usually difficult to measure. Close examination of the radar data shows that the vertical extent of the convergence reaches 2000 to 2500 m and at 1245 LT velocity scans show 55 km h^{-1} away from and 25 km h^{-1} towards the radar with maximum winds of 90 km h^{-1} at 2400 m elevation. These wind speeds are consistent with observations from the Perth radiosonde and lie within the likely depth of plume mixing. The convergence seen on radar is also consistent with the conceptual model of Potter (2012) described above.

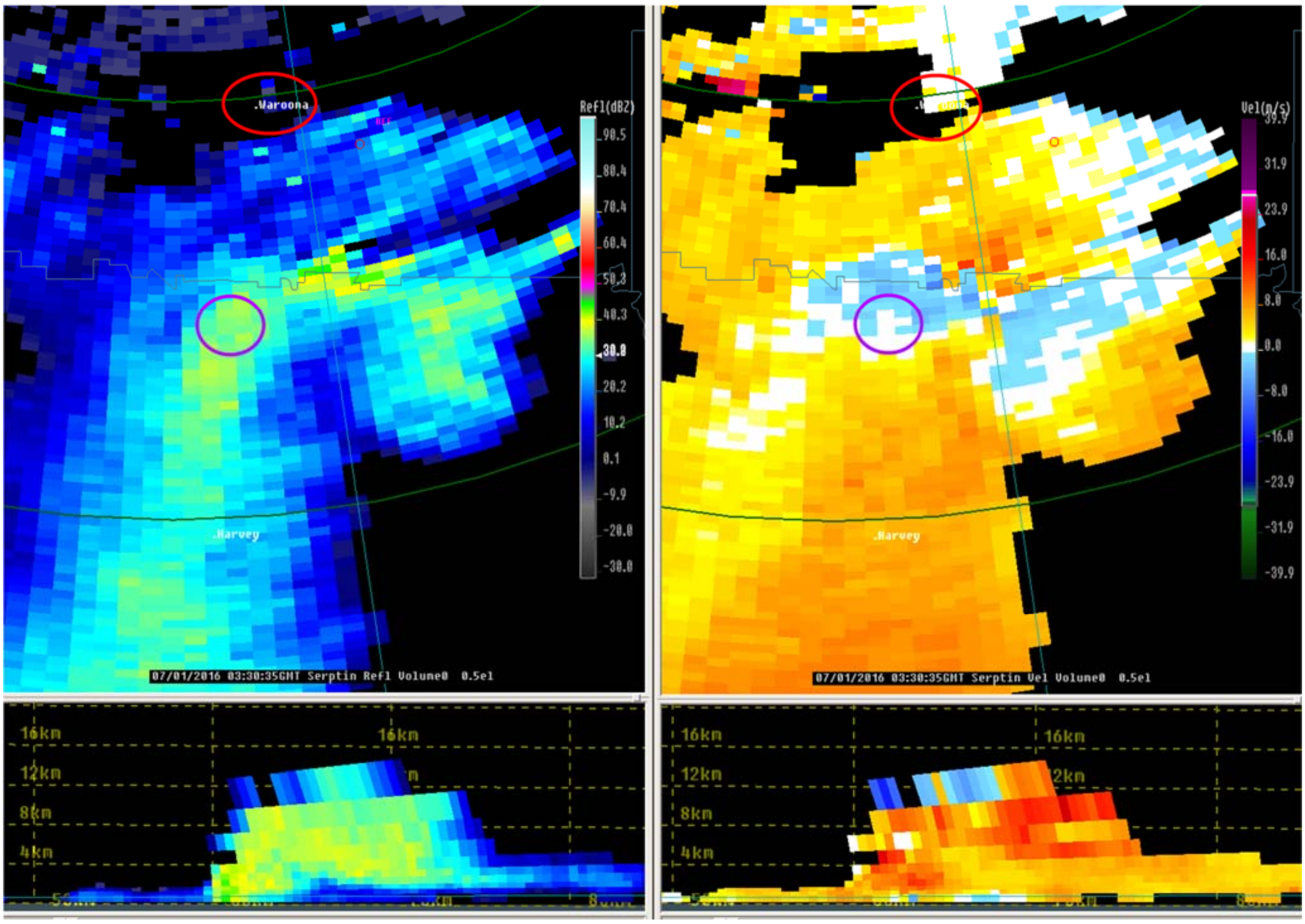

Fig. 15: 3D-Rapic plan view split image showing reflectivity (left) and velocity (right) at 1130 LT 7 January. Red ellipse shows the location of Waroona and purple ellipse shows the location of Yarloop. The convergence zone is the northern interface of the blue (inbound) and yellow/orange (outbound) Doppler velocity returns.

The fire reconstruction (Fig. 2) shows substantial perimeter growth between 0930 and 1330 LT, a period that featured two separate pyroCb pulses. There are several factors that are likely to have contributed to the pyroCb pulses. Firstly, the fire was running through forest that had been unburnt for more than twenty years and consequently had heavy surface fuel loads. Secondly, the fuels had experienced limited overnight fine fuel moisture recovery in the hot, dry conditions, similar to the description of the Pickering Brook fire in Cheney (2010) (fine fuel moisture was eleven-twelve per cent (McCaw et al., 2016)). Thirdly, the fire reconstruction and radar data indicate that the fire was burning on a front around 20 km long (likely with some discontinuities) and the contribution of the fireline orientation perpendicular to above-surface winds and heavy fuels in producing the high integrated instantaneous energy release sufficient to trigger pyroCb cannot be understated.

The radar data returns at 1030 LT were all below 5600 m. Vertical development of the first pulse occurred rapidly and was short-lived between 1120 and 1200 LT with the highest returns reaching 12600 m at 1130 LT. The second pulse can be seen on radar from 1320 LT with returns to 12000 m and lightning strikes between 1330 and 1417 LT. The second pulse was also short lived and weakened quickly, with the rapidly decay of the plume structure consistent with the high wind shear environment. In comparison to the high reflectivities on 6 January that exceeded 50 dBZ, reflectivity returns on 7 January were mostly below 40 dBZ. The second convective pulse was filmed by time lapse photography by Steve Brooks of Perth Weather live https://www.facebook.com/perthweatherlive/videos/1011147718926440/. The video shows rapid development, strong turbulence and shear and a pileus cloud cap above the pyroCb, which is indicative of strong updrafts. The two pyroCb pulses suggest that temporary periods of higher energy release occurred, which were able to overcome an inversion at around 600 hPa (evident on the Perth radiosonde). Possible triggers for the short-lived convective pulses include the fire moving through localised heavier fuels and/or small topographic variations triggering enhanced convergence.

After the second pyroCb peaked at around 1400 LT the fire produced no further convection of note during the afternoon. The timing of the final lightning strike from the pyroCb at 1417 LT is noteworthy as mid-afternoon is the normal time for onset, not cessation of surface-driven thunderstorm activity. Satellite imagery shows development of (non-fire) thunderstorms to the northeast from around 1530 LT.

Extensive defoliation occurred during the late morning and early afternoon fire run, then during the afternoon fire spread slowed and there was a shift from defoliation in a high intensity crown fire to crown scorch. This indicates a decrease in fire intensity, with less convective heat being produced by a less intense fire burning in the surface fuel and understorey shrub layer during the afternoon. It is consistent with the observation that deep pyroconvection above a fire is often associated with crown fire. Contributing factors to pyrocumulus development include the high fuel loads as well as high levels of moisture from a) the combustion process, b) drying of fuels and c) release of free water. The transition in fire intensity was not due to a reduction in wind speed at either Dwellingup or Wagerup AWS. However, winds on the afternoon Perth radiosonde had decreased considerably in the boundary layer and this is consistent with the suggestion that morning fire spread was driven by entrainment of stronger winds by the descending rear inflow jet.

The morning fire run and pyroCb pulses occurred directly beneath a sharp upper trough at 200 hPa with a cut-off upper low further west (see Fig. 16). The ACCESS-Global NWP model indicates weak divergence (not shown) over the fire region. Peterson et al. (2015) describe episodes of pyroconvection, associated fast fire runs and extreme fire behaviour at the Rim Fire that occurred beneath a cut-off low and upper divergence at 250 hPa. Their study concludes that favourable upper level dynamics are a key ingredient for pyroCb development and emphasises that upper level meteorology must be considered when forecasting pyroconvection. Our interpretation of the Waroona fire provides further support for this proposition.

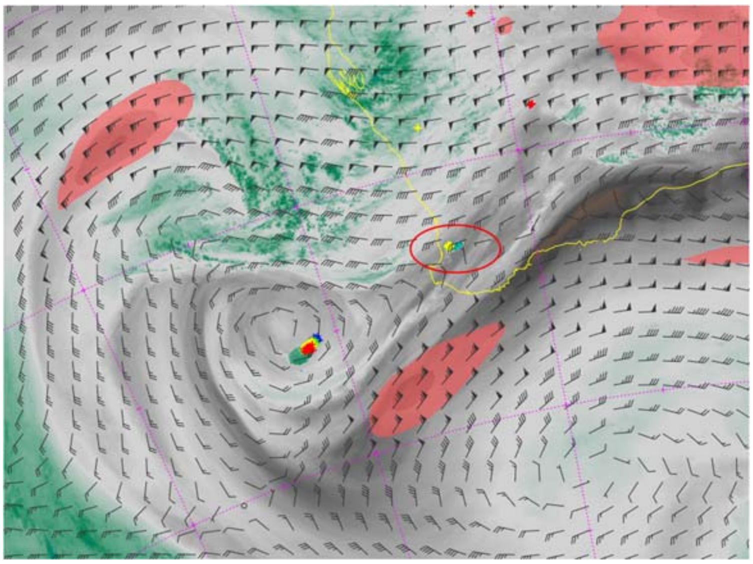

Fig. 16: Water vapour image from Himawari satellite at 0400 UTC overlain with 200 hPa winds from the European Centre for Medium-Range Weather Forecasts operational NWP model. Red ellipse shows fire location and coloured crosses show lightning strikes.

The peak FFDI on 7 January at Dwellingup AWS was 54 at 1613 LT, a time which matched neither the late morning and early afternoon fire run, defoliation and pyroCb development, or the evening ember shower over Yarloop that will be described in the following section.

6. Yarloop ember storm

On the evening of 7 January the fire burnt through the town of Yarloop, causing two fatalities and destroying numerous buildings. The fire activity at Yarloop was associated with massive ember showers. Before 1900 LT fire behaviour was described as `quite mild' (McCaw et al., 2016), as the fire burnt to the east of Yarloop through areas of remnant native forest, pasture and agricultural land. Around 1900 LT, the fire front moved into an area of heavier fuels in nature and crown reserves east of the town, which had been unburnt for longer than twenty years. Shortly after, an ember storm was reported with a large number of buildings ignited. Fire activity escalated dramatically between 1900 and 2030 LT with fire spread of 2000 m h^{-1} (McCaw et al., 2016). Quotes from Operations Officers in Ferguson (2016) include: `The fire just jumped in every direction - north, south, east and west' and `... at one stage every single boundary was a head fire when, you know it went through Yarloop. Like, the whole thing just exploded in a massive downdraft.' The key features of the Yarloop fire were 1) the sudden and dramatic transition in fire behaviour coincident with a move to heavier fuels 2) the massive ember shower and 3) very active fire spread in multiple directions.

The meteorological observations at Wagerup AWS between 1800 and 2100 LT show temperature staying high during the evening (high 30s C) and relative humidity remaining steady around fifteen per cent (see Fig. 14). Wind observations show an increase in easterly wind speed around 1900 LT. Between 1800 and 1900 LT, wind speed averaged 20.5 km h^{-1} with gusts averaging 29 km h^{-1}, then from 1900 to 2000 LT, average wind speed increased to 29.2 km h^{-1} with gusts 41 km h^{-1} and similar conditions were recorded between 2000 and 2100 LT. Observations from Dwellingup showed a similar trend, but slightly less windy.

A reservoir of drier air advected from further east moved across the fire area during the afternoon and evening (Bureau of Meteorology, 2016b). This dry air would contribute to lowering the fine fuel moisture. However, the observed decrease in dew point temperatures occurred over a period of several hours and because of the time lag between changes in environmental relative humidity and fire fuel moisture, the dry air cannot be readily attributed as the dominant factor driving the extremely rapid increase in fire activity. Similarly, the observed 30 per cent increase in wind speed provides only a partial explanation for the increase in fire activity.

The Serpentine radar shows detail of the fire plume dynamics during the evening. Several recent Australian studies of radar data have provided insights into the structure of fire plumes (e.g. Bannister (2014), Bureau of Meteorology (2016a), McCarthy et al. (2016)). The Serpentine radar reflectivity and Doppler velocity scans show several features pertinent to the ember shower over Yarloop. Prior to 1914 LT, returns through the mixed layer were below 3000 m and near-surface velocity data shows light winds 5-15 km h^{-1}. Between 1924 and 1933 LT the radar recorded strong development in the fire plume. At 1933 LT, the height of the plume increased to 7200 m just south of Yarloop. This is a more than doubling in plume height within twenty minutes. The highest returns are coincident with a strongly convergent signature which is shown in Fig. 17. The feature is short lived and extends between approximately 1800 to 3300 m elevation. By 1943 LT the feature had dissipated. The timing of the increase in the peak elevation of radar returns matches the increase in fire activity and the destructive ember shower over Yarloop.

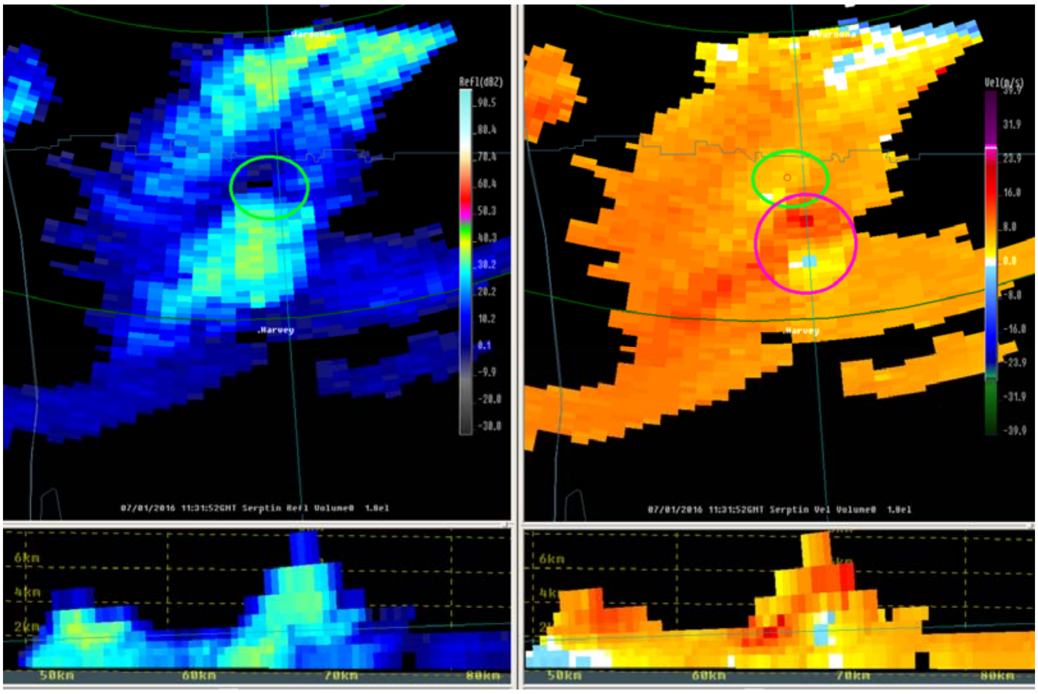

Fig. 17: 3D-Rapic plan view split image showing reflectivity (left) and velocity (right) at 1931 LT 7 January. Green ellipse indicates the approximate centre of the town of Yarloop and pink circle indicates the strong convergent signature in the velocity scan.

ACCESS simulations were run to analyse the meteorology surrounding the Yarloop ember storm. However, these simulations produced a density current outflow that did not verify well against the observations. It appears that the model produced convection to the north of the fire, which did not occur. In the simulations, the convective outflow moved across the fire area, producing cooler conditions and anomalous winds. Because of the poor model verification, the NWP results for Thursday evening are not shown here.

Our analysis of the available data suggests that the ember storm that destroyed the town of Yarloop was triggered by plume interaction with downslope winds and the vertical development may have been enhanced by the presence of a hydraulic jump, similar to the situation at Waroona the previous evening, but enhanced by the heavy fuels east of the town. Downslope winds are a known local meteorological effect at Yarloop ... `The occurrence of evening downslope winds is a feature that numerous locals have observed and remarked on in this Special Inquiry' (Ferguson, 2016). The increase in wind speed at Wagerup between 1800 and 1900 LT is consistent with onset of downslope winds. However, the steady increase in wind speed seen on the AWS is disproportionate with the sudden, dramatic increase in fire activity. This apparent discrepancy can be reconciled by examining the vertical atmospheric structure driving downslope winds and by considering how the fire plume may interact with a hydraulic jump, particularly when combined with an increase in energy release resulting from the transition into heavier fuels along the eastern boundary of the town. The increase in energy release when the fire moved into heavier fuels may have produced a transition from the fire burning in a shallow near-surface layer to the plume extending through a greater depth of the boundary layer.

The hydraulic jump region is located adjacent to the lee slope and is associated with strong vertical motion that can reach to heights of several thousand feet. Pitts and Lyons (1989) conducted an experiment with an aircraft taking wind and turbulence observations adjacent to the Perth scarp. The observations from a series of transects own on 3 February 1987 show development of a hydraulic jump region that suggests the wave amplified suddenly in the hour between transect runs, indicating the onset of downslope winds can occur very rapidly. An additional known ingredient for enhanced turbulence can be seen on the 2000 LT Perth radiosonde; a reversal in wind direction or `critical level' near 12,000ft. A particular feature of the structure of the hydraulic jump is the wave-like structure of upmotion and compensating downmotion and the downwards acceleration is consistent with the description in Ferguson (2016) of `... the whole thing just exploded in a massive downdraft.'

We hypothesize that on 7 January, as the fire approached the east of Yarloop and moved into an area of heavier fuels, downslope winds and an associated hydraulic jump may have developed. It is also possible the fire moved into a `hot spot' region of stronger downslope winds. The increase in energy release from the heavier fuels could increase the vertical extent of the fire plume, which then has potential to produce a feedback loop due to the plume interacting with the stronger winds above the surface and the jump region. This could create a strongly turbulent vertical structure, which would then provide an enhanced mechanism for lofting of firebrands that were produced by the heavier fuels just east of the town. The process accounts for the rapid and destructive ember shower over Yarloop.

7. Summary

The Waroona fire burnt 69,000 ha south of Perth on 6 and 7 January 2016 with devastating consequences for the towns of Waroona and Yarloop and the broader community of Western Australia. A year later, media reports continue to describe a community struggling to understand how the fire burnt so fast and with such intensity, and devastated by its impacts. This case study examined the meteorology and fire behaviour in detail and identified processes that are likely to have contributed to the extreme fire behaviour that occurred. Although the study is necessarily somewhat speculative as a consequence of data limitations, the findings present a cohesive narrative that links the observations with known meteorological processes.

During the first two days of the fire there were four periods of particular interest. On the evening of 6 January and around midday 7 January pyroCb developed over the fire. The pyroCb on 6 January was multicellular and developed a deep plume to higher than 14 km and an extensive cirrus anvil, consistent with stratospheric intrusion. Lighting from the pyroCb was observed to ignite new fires downwind of the main fire front and a density current outflow was observed at Wagerup AWS nearby. On the evening of 6 January the town of Waroona was reported to be under ember attack. The ember attack is likely to have resulted from lightning ignition of a new fire closer to the town, which was subsequently driven by a density current outflow produced by the pyroCb. Local downslope winds and the presence of a hydraulic jump provided a localised lofting, transport, and turbulent dispersion mechanism for firebrands from the new fire, and this produced the ember attack over Waroona. The pyroCb on 7 January was attributed to momentum entrainment from a low level jet and high energy release along a 20 km fireline. The convection featured two transient pulses that overcame a weak elevated temperature inversion and strong updrafts produced a pileus cloud cap above the pyroCb. The evening ember storm that destroyed the town of Yarloop on 7 January was also driven by downslope winds, similar to the ember attack over Waroona the previous evening. Heavy, long unburnt fuels to the east of the town were a significant contributing factor to the intensity of the fire as well as a source of firebrands. Doppler radar velocity scans show significant vertical plume development and localised convergence at the time Yarloop was destroyed by the ember shower.

8. Conclusions

In conclusion, we will consider how the main findings from the Waroona fire may be applied to future events by meteorologists and fire analysts so that similar fire escalation may be anticipated in advance, allowing for mitigation against the impacts of fire activity. Some `watch-out' environments where the situation may be conducive to a transition to extreme fire behaviour are summarised below.

A key finding from the examination of the Waroona fire environment is that the highly turbulent low-level wind environment associated with downslope winds most likely triggered the destructive evening ember storms over Waroona and Yarloop. The fire burning near the hydraulic jump provided an enhanced mechanism for localised transport and deposition of large quantities of firebrands. This, combined with the transition to heavier fuels favourable for firebrand production resulted in an environment favourable for rapid plume development, ember showers and anomalous rapid fire spread. This is highly relevant for Australian fires as there are many locations where downslope winds occur, including the Mount Lofty Ranges in South Australia and the Darling Scarp in Western Australia, both of which have large populations and heavy loads of flammable vegetation. Recent research into the dynamics of fire plumes (e.g. Thurston et al. (2017)) shows that the turbulence within a fire plume is a critical component of the spotting process and a determinant of landing distribution and ember dispersal and evidence from the Waroona fire shows that a highly turbulent low-level wind environment is favourable for destructive ember showers.

Local knowledge of such downslope wind regimes may be critical information at firegrounds. This local knowledge should be complemented by detailed examination of Numerical Weather Prediction (NWP) operational output, as simulations run at sufficiently high resolution can resolve the downslope mechanism. In particular, interpretation of cross sections of wind vectors and potential temperature from NWP output can identify the presence of hydraulic jumps. The simulations shown here resolved the hydraulic jump at a model resolution of 1.3 km, and operational model runs at 4 km resolution usually identify the stronger winds. The likelihood of downslope winds developing can also be assessed by considering the strength of the pressure gradient across a region as well as the presence, height and strength of a temperature inversion above or near the level of the ridge top.

The effect of topographic wind modification and fire interaction is usually assessed over high terrain, especially steep mountain ranges (e.g. Sharples et al. (2010)). However, there are cases of extreme fire behaviour triggered by wind flow over terrain of just a few hundred metres, so identifying fires burning over relatively low relief topography as having potential to develop dynamic fire behaviour may provide an early warning. As downslope winds develop on and near the base of the leeward slopes of ranges, the risk of escalation for fires burning in these areas may not be identified, as a conventional assessment would identify the windward slope as more exposed to stronger winds and consequently having higher fire risk. The potential for unusual fire activity is exacerbated by unstable atmospheric environments and by fire-modified winds (e.g. Simpson et al. (2014), Sharples et al. (2013) and references contained therein).

The two pyroCb events provide differing look-outs for future fires. The pyroCb on 6 January was multicellular, with spatially separated updrafts and downdrafts. The gust recorded at Wagerup AWS on the evening of 6 January shows the potential hazard associated with pyroCb downdrafts. As density currents from thunderstorm outflows can last for tens of minutes (e.g. Thurston et al. (2015)), and the outflow boundary is a region of enhanced turbulence, they are favourable location for transport of large quantities of embers, as well as a sustained period of anomalously fast and erratic fire spread. The development of pyroCb on the morning of 6 January was linked to the long fire line and deep flaming zone in heavy fuels; this produced a high instantaneous energy release over a large area. Long fire lines should be watch-out for deep pyroconvection.

The risk of lightning ignition from pyroCb starting new fires downstream has similarities to the risk of spot fire ignitions from lofted firebrands in the plume, however the area at risk differs. Dowdy and Mills (2012) present a study on fires ignited by lightning in Victoria, Australia, in which they find the most common month for lightning ignitions to occur is January and the average chance of fire per stroke in that month is 0.7 per cent (0.4 per cent across all months). This is consistent with analysis of fire reports from the Warren region in Western Australia, where lightning ignition was also most common in January (McCaw and Read, 2012). The report on the Chisholm firestorm (Rosenfeld et al., 2007) states that pyroCb are characterised by high-intensity positive lightning strikes (compared to normal storms that have a higher proportion of negative strikes). Positive cloud-to-ground ashes are more energetic (than negative strikes) and the current persists for longer, increasing the potential to ignite new fires. The potential for pyroCb to ignite new fires downstream should be monitored.

The Doppler radar provided insights into the plume structure and fire- modified winds. Radar data from Laverton in Victoria provided insights into the fire behaviour on Black Saturday (Bannister, 2014) and Buckland Park radar in South Australia was used in real-time for prediction during the Pinery fire (Bureau of Meteorology, 2016a). The Waroona fire was the first major fire to burn close to the Serpentine radar since its installation and the close proximity to the Doppler radar provided detail of the structure of the plume as well as the convergence produced by the fire-modified winds. Current research (McCarthy et al., 2016) is showing the potential for deployment of truck-mounted radar at fires and it is likely that portable radars will be located near fires more frequently in the future. This raises questions on how best to use radar data; firstly, for real time monitoring and diagnosis and secondly, for understanding the dynamics of fire plumes. Fires that burn in proximity to radars should be closely monitored on both reflectivity and velocity scans (where available), and skilled interpretation may contribute to real time fire intelligence and provide input into critical fireground decisions.

The fire reconstruction (McCaw et al., 2016) shows both pyroCb episodes were associated with extensive defoliation by crown fire. Whether or not there is a correlation between deep pyroconvection and crown fires has not been established in the scientific literature; however, anecdotal evidence suggests links between defoliation or crown scorch and an unstable atmosphere, even in unremarkable wind and temperature conditions. The Hovea fire, which is described in Mills and McCaw (2010) provides an example. The Hovea fire had unusual levels of crown scorch for relatively benign burning conditions, with evidence of heightened instability. The link between crown scorch and atmospheric instability is an avenue worth further investigation.

The extreme fire behaviour at Waroona occurred against normal diurnal trends and observations show the observed values of FFDI do not correlate with periods of extreme fire activity. A contributing factor to the disparity was morning and evening entrainment of strong low level winds by two processes; mixing down from a low level jet and downslope enhancement. Entrainment of both momentum and dry air from above the surface to a fire can occur by either dynamic atmospheric processes (e.g. Mills (2008)) or by fire-atmosphere feedback. Although the response of the fire to entrainment of air with higher wind speeds will be instantaneous, the response to changes in atmospheric moisture will be lagged due to the fuel moisture response time. Therefore, the effects of momentum entrainment will dominate over dry air entrainment. Consequently, the potential for strong winds above the surface to be mixed down behind the plume and increase fire spread should be assessed.

Ferguson (2016) emphasises that experienced fire managers were surprised by the fire activity. The fire reconstruction prepared in McCaw et al. (2016) highlights discrepancies between observed and predicted spread at several stages of the fire. The discrepancies are between the observed (reconstructed) spread derived from field observations (e.g. leaf freeze) and the predicted spread calculated from algorithms using fuel data and weather observations as inputs. This illustrates a challenge in anticipating fire behaviour as the discrepancy in the report of McCaw et al. (2016) shows that any predictive model using near-surface environmental winds as an input and with an underlying quasi-steady state assumption of spread would not correctly predict the spread of the Waroona fire. This will hold irrespective of whether calculations were made by hand or using a two dimensional fire spread simulator on a computing platform.

The analysis presented in this paper contributes substantially to the identification of processes that caused the Waroona fire to burn the way it did. This highlights that any approach using near-surface environmental winds as input to predictions of fire spread will be of limited accuracy in certain cases. Fire prediction tools underpinned by quasi-steady state assumptions and driven by environmental near surface winds have no capacity to identify environments conducive to pyroCb development, plume processes, momentum entrainment or dynamic fire spread or of fire-modified winds causing anomalous fire spread.

Dynamic fire behaviour has contributed to many fire fatalities and is in many cases linked to fire-atmosphere interactions, particularly in mountainous terrain. The triggers and thresholds relating dynamic fire behaviour and the role of critical thresholds in weather, terrain and fuels and combinations of these therefore require further research and understanding to enable provision of better intelligence to Incident Management Teams tasked with protection of life and property during these events.

9. Acknowledgements

Many people have contributed towards the preparation of this manuscript and their input is much appreciated. Thanks to Harald Richter for sharing his thunderstorm and radar expertise. Thanks to Hank de Wit for helping prepare Figures 1 and 2. Thanks to several members of `pyrocb@yahoogroups.com' for their thoughts and data provision for the pyroCb events. Thanks to Tony Bannister, Paul Fox-Hughes, Brian Potter and an anonymous reviewer for their thoughtful and constructive reviews, which have much improved the paper. The support of the Commonwealth of Australia through the Cooperative Research Centre program is acknowledged.

10. References

Bannister, T. (2014). Black Saturday 2009: A radar view of the Kilmore East fire. CAWCR Research Letters, Issue 11, Centre for Australian Weather and Climate Research, Australian Government Bureau of Meteorology.

Blockley, J.A. and Lyons, T.J. (1994). Airflow over a two-dimensional escarpment. II: Nonhydrostatic flow. *Quarterly Journal of the Royal Meteorological Society*, 120:79-109.

Bureau of Meteorology (2016a). Meteorological aspects of the Pinery Fire on 25 November 2015. Australian Government Bureau of Meteorology, South Australian Regional Office.

Bureau of Meteorology (2016b). Meteorological aspects of the Waroona Fire January 2016. Australian Government Bureau of Meteorology, Western Australian Regional Office.

Cheney, N.P. (2010). Fire behaviour during the Pickering Brook wildfire, January 2005 (Perth Hills Fires 71-80). Conservation Science Western Australia, 7 (3):451-468.

Department of Environment and Conservation (2011). Wagerup 2009 Air Quality Study. Government of Western Australia.

Dowdy, A.J. and Mills, G. (2012). Atmospheric and Fuel Moisture Characteristics Associated with Lighting-Attributed Fires. *Journal of Applied Meteorology and Climatology*, 51 (11):2025-2037.

Ellis, P.F.M. (2013). Firebrand characteristics of the stringy bark of messmate (*Eucalyptus obliqua*) investigated using non-tethered samples. *International Journal of Wildland Fire*, 22:642-651.

Ferguson, E. (2016). Reframing Rural Fire Management: Report of the Special Inquiry into the January 2016 Waroona Fire. Government of Western Australia.

Goens, D.W. and Andrews, P.L. (1998). Weather and fire behaviour factors related to the 1990 Dude Fire near Payson, Arizona. In `Proceedings, 2nd Symposium on Fire and Forest Meteorology', 11-16 January 1998, Phoenix, AZ. (American Meteorology Society, Boston).

Grace, W. and Holton, I. (1990). Hydraulic jump signatures associated with Adelaide downslope winds. *Australian Meteorological Magazine*, 38:43-52.

Johnson, R.H., Schumacher, R.S. and Ruppert, Jr., J. H. (2014). The Role of Convective Outflow in the Waldo Canyon Fire. *Monthly Weather Review*, pages 3061-3080.

Kepert, J.D. and Smith, R.K. (1992). A Simple Model of the Australian West Coast Trough. *Monthly Weather Review*, 120:2042-2055.

Krumm, W.R. (1954). An explanation of the meteorological conditions which probably caused unexpected behaviour of the Rattlesnake Fire, Mendocino National Forest, July 9, 1953. Unpublished report.

McCarthy, N., McGowan, H. and Guyot, A. (2016). The bushfire convective plume experiment: mobile radar observations of pyroconvection from the Mt Bolton fire, 2016. Report No. 2016.199, Bushfire and Natural Hazards Cooperative Research Centre.

McCaw, L., Burrows, N., Beecham, B. and Rampant, P. (2016). Reconstruction of the spread and behaviour of the Waroona bushfire (Perth Hills 68) 6-7 January 2016. Government of Western Australia Department of Parks and Wildlife.

McCaw, L. and Read, M. (2012). Lightning fire ignitions in the Warren Region of south-west Western Australia, 1977-2012. In Delegate Handbook AFAC 12: Diverse country, common ground, Perth 28-31 August 2012, page p 54.

Mills, G. (2008). Abrupt surface drying and fire weather Part 1: overview and case study of the South Australian fires of 11 January 2005. *Australian Meteorological Magazine*, 57:299-309.

Mills, G. and McCaw, L. (2010). Atmospheric Stability Environments and Fire Weather in Australia: Extending the Haines Index. CAWCR Technical Report No. 20, Centre for Australian Weather and Climate Research.

Peace, M., Mattner, T., Mills, G., Kepert, J. and McCaw, L. (2015a). Fire modified meteorology in a coupled fire-atmosphere model. *Journal of Applied Meteorology and Climatology*, 54:704-720.

Peace, M., Mattner, T., Mills, G., Kepert, J. and McCaw, L. (2016). Coupled Fire-Atmosphere Simulations of the Rocky River fire using WRF-SFIRE. *Journal of Applied Meteorology and Climatology*, 55:1151-1168.

Peace, M., McCaw, L.W., Kepert, J.D., Mills, G.A. and Mattner, T. (2015b).
WRF and SFIRE simulations of the Layman fuel reduction burn. *Australian Meteorological and Oceanographic Journal*, 65:3-4:302-317.

Peterson, D.A., Hyer, E.J., Campbell, J.R., Fromm, M.D., Hair, J.W., Butler, C.F. and Fenn, M.A. (2015). The 2013 Rim Fire: Implications for Predicting Extreme Fire Spread, Pyroconvection, and Smoke Emissions. *Bulletin of the American Meteorological Society*, 96 (2):229-247.

Pitts, R.O. and Lyons, T.J. (1989). Airflow over a two-dimensional escarpment. I: Observations. *Quarterly Journal of the Royal Meteorological Society*, 115:965-981.

Pitts, R.O. and Lyons, T.J. (1990). Airflow over a two-dimensional escarpment. II: Hydrostatic flow. *Quarterly Journal of the Royal Meteorological Societ*y, 116:363-378.

Potter, B. (2012). Atmospheric interactions with wildland fire behaviour - II. Plume and vortex dynamics. International *Journal of Wildland Fire*, 21:802-817.

Rosenfeld, D., Fromm, M., Trentmann, J., Luderer, G., Andreae, M.O. and Servranckx, R. (2007). The Chisholm firestorm: observed microstructure, precipitation and lightning activity of a pyro-cumulonimbus. *Atmospheric Chemistry and Physics*, 7:645-659.

Rothermel, R.C. (1991). Predicting behaviour and size of crown fires in the northern Rocky Mountains. USDA Forest Service, Intermountain Research Station, Research Paper, INT-438:46.

Sha, W., Physick, W. and Grace, W. (1995). A Numerical Experiment on the Adelaide Gully Wind of South Australia. *Mathematical and Computer Modelling*, 21 (9):119-123.

Sharples, J.J., Mills, G.A., McRae, R.H.D. and Weber, R.O. (2010). Foehn-Like Winds and Elevated Fire Danger Conditions in Southeastern Australia. *Journal of Applied Meteorology and Climatology*, 49:1067-1095.

Sharples, J.J., Simpson, C.C. and Evans, J.P. (2013). Examination of wind speed thresholds for vorticity-driven lateral fire spread. MODSIM 2013, 20th International Congress on Modelling and Simulation., pages 263-269.

Simpson, C.C., Sharples, J.J. and Evans, J.P. (2014). Resolving vorticity driven lateral fire spread using the WRF-Fire coupled atmosphere-fire numerical model. *Natural Hazards and Earth System Sciences*, pages 2359-2371.

Sullivan, A.L. (2017). Inside the Inferno: Fundamental Processes of Wildland Fire Behaviour. Part 2: Heat Transfer and Interactions. Current Forestry Reports, 3:150-171.

Thurston, W., Kepert, J.D., Tory, K.J. and Fawcett, R. J. B. (2017). The contribution of turbulent plume dynamics to long-range spotting. *International Journal Wildland Fire*. In revision.

Thurston, W., Tory, K.J., Fawcett, R.J.B. and Kepert, J.D. (2015). Large-eddy simulations of pyroconvection and its sensitivity to environmental conditions. Research proceedings from the Bushfire and Natural Hazards CRC and AFAC Conference, M Rumsewicz (ed.), Bushfire and Natural Hazards CRC, 148-160, ISBN: 978-0-994 1696-5-5.

Tolhurst, K.G., Chatto, K., Leggett, T. and Treloar, A. B. A. (1999). Development, behaviour, threat and meteorological aspects of a plume-driven bushfire in west-central Victoria: Berringa fire February 25-26, 1995. Creswick Research Station, Fire Management, Department of Natural Resources and Environment.

Yarnell Serious Accident Investigation Team (2013). Yarnell Fire Serious Accident Investigation Report. Arizona State Forestry Division, State of Arizona.